

## EQUIVALENT CIRCUIT MODEL OF SEMICONDUCTOR LASERS TAKING ACCOUNT OF GAIN SUPPRESSION

Kambiz Abedi and Mohsen Khanzadeh

Department of Electrical Engineering, Faculty of Electrical and Computer Engineering,  
Shahid Beheshti University, G. C., Evin 1983963113, Tehran, Iran

### ABSTRACT

*In this paper, the rate equation-based equivalent lumped element circuit model of semiconductor lasers is used to study the effect of gain suppression on characteristics of intensity modulation of small signal of Fabry perot-semiconductor lasers (FP-SLs). Modeling is firstly performed with the simple solution of rate equations of semiconductor lasers (SL), which can be used to model basic laser behavior under both direct current (DC) and alternating current (AC) conditions. Then the model is implemented in conventional simulation program with integrated circuit emphasis (SPICE) circuit simulators, such as advanced design system (ADS), and it is used to simulate the small signal intensity modulation features of FP-SLs. The results of circuit simulations are compared with those of numerical simulations. This simple theoretical model is especially suitable for computer aided design (CAD), and greatly simplifies the design of optical communication systems.*

**KEYWORDS:** *Equivalent Circuit Model, Semiconductor Lasers, Gain Suppression.*

### I. INTRODUCTION

There has been growing interest in developing direct modulation of semiconductor diode in high speed and long haul optical communication systems over the past decade. Moreover a major advantage of semiconductor lasers is that they can be directly modulated. In contrast, many other lasers are continuous wave sources and cannot be modulated directly at all. The other advantages of semiconductor lasers are including their low cost, compact size, low power consumption and high optical output power [1, 2]. On the other hand, when the laser is biased above threshold its operation and dynamics are influenced by property of gain suppression, which originates from intra-band relaxation processes of injected carriers [3]. For instance the damping rate of laser relaxation oscillations and modulation bandwidth are determined by gain suppression [2].

Building an accurate laser diode model becomes more important in modern high-speed optoelectronic integrated circuit (OEIC) design. Various efforts have been made to get a well-established laser models such as a rate equation-based model and a finite-difference time-domain (FDTD)-based model for OEIC design, however, the difficulty of extracting accurate model parameters in the rate equation-based model case and the long simulation time in the FDTD-based model remain major obstacles to applying them to actual OEIC design [4].

Accurate extraction of the small signal equivalent circuit for laser diodes (LDs) is extremely important for optimizing the device performance. The rate-equation model parameters can be obtained from modulation response by using numerical optimization techniques. However, the accuracy of the numerical optimization methods - that minimize the difference between measured and modeled data can vary depending upon the optimization method and starting values, while the analytical methods allow us to extract the equivalent circuit model parameters in a straightforward manner [5].

The theoretical work presented here is based on the simulation model proposed by Ahmed et al. [6]. Then based on the result of theoretical analysis of rate equations, small signal equivalent circuit model of InGaAsP semiconductor lasers is proposed. Because the main goal of this work is establishing a

Fabry perot-semiconductor lasers (FP-SLs) model that can be used in computer aided design (CAD) of optoelectronic systems, we try to implement this model in simulation program with integrated circuit emphasis (SPICE)-like simulators. Then we can simulate the FP-SLs combined with other electrical devices such as laser drivers. The realization of SPICE simulation depends on the transformation from the model equations into the equivalent circuit representation.

The solution of this equivalent circuit model is compared with the numerical simulations done by MATLAB software and the results presented by Ahmed et al. [6]. To the author's knowledge, reports on the evaluation of gain suppression in circuit model of semiconductor lasers have not been yet reported. This paper is structured as follows. Theoretical solutions of rate equations are introduced in Section 2. In Section 3, Rate equation-based model is investigated. The results and discussion of this work appear in Section 4. Finally, Section 5 contains the conclusion.

## II. THEORETICAL SOLUTIONS OF RATE EQUATIONS

The equivalent circuit model is based on the theoretical solution of rate equations. Derivation of these equations originates from Maxwell equations with a quantum mechanical approach for the induced polarization [4].

However, the rate equations could also be derived by considering physical phenomena. Through this approach, the rate equations with the number of injected electrons into the active layer  $N(t)$ , through the current  $I(t)$  and photon number  $S(t)$  are given by [2]:

$$\frac{dN}{dt} = \frac{1}{e} I(t) - AS - \frac{N}{\tau_e} \quad (1)$$

$$\frac{dS}{dt} = (G - G_{th})S + \frac{C}{\tau_r} N \quad (2)$$

Equation (1) relates the rate of change in the electron number to the drive current  $I(t)$ , the stimulated photon number  $S$  and carrier recombination rate. Equation (2) associates the rate of change in photon number to photon loss and the rate of coupled recombination into the lasing mode.

$G$  in the Eq. (2) is the optical gain ( $s^{-1}$ ), and is defined in the nonlinear form as [2]:

$$G = A - BS \quad (3)$$

With the coefficients of linear gain  $A$  and nonlinear gain (gain suppression)  $B$  defined as [7]:

$$A = \frac{a\zeta}{V} (N - N_g) \quad (4)$$

$$B = \frac{9}{2} \frac{\pi c}{\epsilon_0 n_a^2 \hbar \lambda_0} \left( \frac{\zeta \tau_{in}}{V} \right)^2 a |R_{cv}|^2 (N - N_s) \quad (5)$$

where  $a$  is the tangential gain,  $\zeta$  is the confinement factor of the optical field in the active layer with volume of  $V$  and refractive index of  $n_a$ ,  $N_g$  is the electron number at transparency,  $N_s$  is the electron number characterizing  $B$ ,  $\tau_{in}$  is the intra-band relaxation time,  $c$  is the Speed of light in free space,  $R_{cv}$  is the dipole moment,  $\hbar$  is the reduced Planck's constant and  $\lambda_0$  is the dielectric constant in free space.  $\lambda_0$  is the lasing wavelength and for this FP-SL is assumed 1.55  $\mu\text{m}$ .

The nonlinear gain coefficient ( $B_0$ ) is approximately calculated and set to a value of 683  $s^{-1}$  [6]. Influence of gain suppression on modulation characteristics is examined by varying the coefficient  $k$  in Eq. (6) to adjust value of  $B$  relative to the fixed value  $B_0$ .

$$B = kB_0 \quad (6)$$

Exact analytical solution of the full rate equations cannot be obtained. Therefore some approximations are needed to find analytical solutions. It is possible to assume that the dynamic changes in the electron and photon number away from their steady-state values are small. Under this assumption, the

small-signal responses of one variable in terms of a perturbation to another can be expressed by taking the differential rate Eqs [4].

$$I(t) = I_b + I_m \cos(\Omega_m t) \quad (7)$$

$$S(t) = S_b + S_m \cos(\Omega_m t) \quad (8)$$

$$N(t) = N_b + N_m \cos(\Omega_m t) \quad (9)$$

where  $I_b$ ,  $N_b$ , and  $S_b$  are the bias components, and  $I_m$ ,  $N_m$ , and  $S_m$  are the magnitudes of the corresponding small-signal perturbations.

By substituting Eqs.(7)–(9) into rate Eqs.(1) and (2), separating equations of both bias and modulation terms, applying several numerical operations, derivations of coefficients, and neglecting the terms of higher harmonics, following pair of equations for the bias components are obtained [6]:

$$\{A_b - BS_b - G_{th}\}S_b + \frac{C}{\tau_r} N_b = 0 \quad (10)$$

$$A_b S_b + \frac{N_b}{\tau_e} - \frac{I_b}{e} = 0 \quad (11)$$

And another pair of linear equations for the modulation components as [6]:

$$\{\Gamma_S + j\Omega_m\}S_m - \frac{a\zeta}{V} \left( S_b + \frac{CV}{a\zeta\tau_r} \right) N_m = 0 \quad (12)$$

$$A_b S_m + \{\Gamma_N + j\Omega_m\}N_m - \frac{I_m}{e} = 0 \quad (13)$$

where  $A_b$  the bias component of linear gain  $A$  is [6]:

$$A_b = \frac{a\zeta}{V} (N_b - N_g) \quad (14)$$

$\Gamma_S$  and  $\Gamma_N$  are the damping rates of  $S(t)$  and  $N(t)$ , respectively, and are given by [6]:

$$\Gamma_S = BS_b + \frac{CN_b}{\tau_r S_b} \quad (15)$$

$$\Gamma_N = \frac{a\zeta}{V} S_b + \frac{1}{\tau_e} \quad (16)$$

### III. RATE EQUATION-BASED MODEL

#### 3.1 Modeling bias components

In this paper, equivalent circuit model is derived from the solution of rate equation for FP-SL, which has the advantage of simple implementation of model and short simulation time. FP-InGaAsP Semiconductor Laser emitting at wavelength  $\lambda = 1.55 \mu\text{m}$  are considered in the calculations. Typical values of the parameters used in modeling and simulations are listed in Table 1.

At the first step, it is necessary to determine the value of threshold current, which specify the lower limit of injected current. When the SL is biased above the threshold, the electron number  $N(t)$  is clamped just above the threshold electron number  $N_{th}$  hence the threshold number of carriers simply determined by [2]:

$$N_{th} = N_g + \frac{G_{th}V}{a\zeta} \quad (17)$$

And consequently the threshold current is calculated from the following relation [2]:

$$I_{th} = \frac{eN_{th}}{\tau_e} \quad (18)$$

**Table 1** Typical value of the parameters of a 1.55 μm InGaAsP laser

| Symbol          | Meaning                                      | Circuit Parameter | Value                     |
|-----------------|--|-------------------|---------------------------|
| e               | Electron charge                              | eI                | 1.6x10 <sup>19</sup>      |
| τ <sub>e</sub>  | Electron lifetime                            | t_e               | 2.83x10 <sup>9</sup>      |
| G <sub>th</sub> | Threshold gain                               | G <sub>th</sub>   | 7.81x10 <sup>10</sup>     |
| a               | Tangential gain coefficient                  | a                 | 7.85<br>×10 <sup>12</sup> |
| ζ               | Field confinement factor in the active layer | zeta              | 0.2                       |
| V               | Volume of the active region                  | V                 | 60x10 <sup>18</sup>       |
| N <sub>g</sub>  | Electron number at transparency              | N <sub>g</sub>    | 5.31x10 <sup>7</sup>      |
| B <sub>0</sub>  | Nonlinear gain                               | B                 | 683                       |
| C               | Spontaneous emission factor                  | C                 | 2.5x10 <sup>5</sup>       |
| τ <sub>r</sub>  | Radiative recombination lifetime             | t_r               | 7.772x10 <sup>9</sup>     |

Substituting G<sub>th</sub> from Table 1 into Eq. (17) and then using the result of N<sub>th</sub> in the Eq. (18) leads to I<sub>th</sub> = 3.33 mA. By solving the Eqs.(10) and (11), the bias component of the photon number (S<sub>b</sub>) can be evaluated as:

$$S_b = \frac{(I_b - I_{th})}{eG_{th}} \quad (19)$$

To obtain a circuit model for bias components of SL, one straight approach is to define a circuit with two nodes, one represents electron number N<sub>b</sub> and the other is for modeling photon number S<sub>b</sub>, so the nodes are labeled with N<sub>b</sub> and S<sub>b</sub>, respectively.

The solution of this circuit and finding the voltages of two above mentioned nodes is equal to calculate the values of bias components S<sub>b</sub> and N<sub>b</sub>. It's obvious that two KCL equations are required to completely describe the circuit. Equation (19) is one of the requisite equations, and by moving toward the KCL equation, it can be rearranged as:

$$\frac{S_b}{R_1} + I_{th} = I_b \quad (20)$$

which R<sub>1</sub> is defined as 1/(e\*G<sub>th</sub>), and due to characteristic of the KCL equation, all components of this expression are current. So three branches are intersected at node S<sub>b</sub> and each one must through amount of current corresponding to each term of the Eq. (20), as illustrated in Figure 1.

The other necessary equation for simulating N<sub>b</sub> is acquired from Eq. (11), by normalizing with a coefficient of 'e' and substituting Eq. (14) it provides:

$$GS_b + \frac{N_b}{R_2} + \frac{N_b}{R_3} - I_b = 0 \quad (21)$$

where R<sub>3</sub> is defined as 1 / (azV\*e\*S<sub>b</sub>) and R<sub>2</sub> is equal to τ<sub>e</sub>/e while azV is defined as a constant factor a ζ /V and G is equal to e\*azV\*N<sub>g</sub>.

In this research, models of bias and small signal equations are implemented using the Hewlett Packard Advanced Design System (HP-ADS) symbolically defined devices (SDDs) model to InGaAsP Fabry-Perot lasers. The benefit of the SDD is that once the model is defined, any circuit simulator in Advanced Design System can use the model, and derivatives are also calculated automatically in the process of simulation.

These kinds of models need the physical parameters of the laser diodes. Thus, the parameters for the equivalent circuit in Figure 1 should be known before making a model. These parameters are shown in Figure 2.

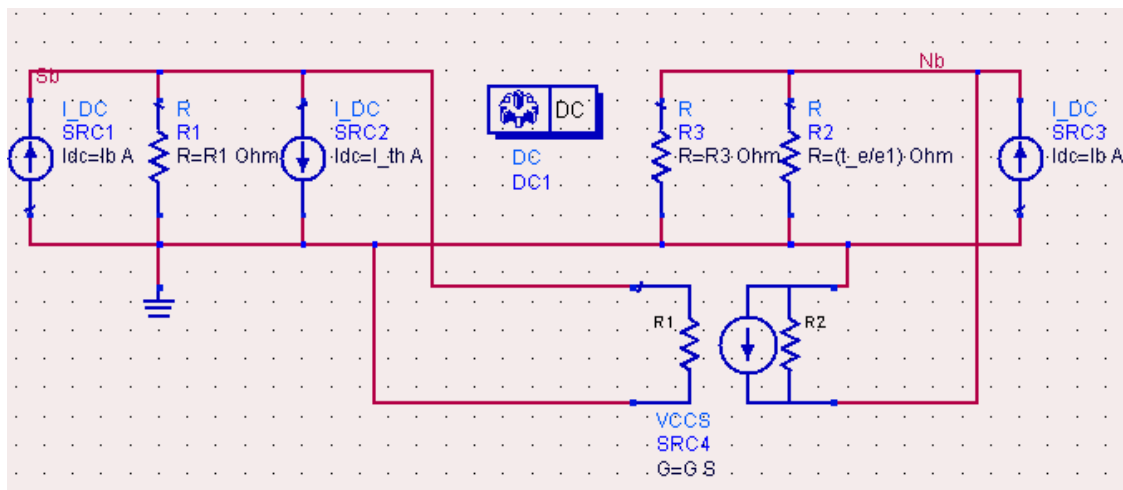


Figure 1. Equivalent circuit model for bias components

| VAR Eqn | VAR             | VAR Eqn | VAR  |
|---------|-----------------|---------|--|
|         | VAR1            |         | VAR9                                       |
|         | $e1=1.6e-19$    |         | $I\_th=e1I\_e*(Gth*V/(a*zeta)+Ng)$         |
|         | $t\_e=2.83e-9$  |         | $Ib=3*I\_th$                               |
|         | $Gth=7.81e10$   |         | $azV=a*zeta/V$                             |
|         | $a=7.85e-12$    |         | $G=e1*azV*Ng$                              |
|         | $zeta=0.2$      |         | $R1=1/(e1*Gth)$                            |
|         | $V=60e-18$      |         | $Sbias=(Ib-I\_th)*R1$                      |
|         | $Ng=5.31e7$     |         | $R3=1/(azV*e1*Sbias)$                      |
|         | $B=683$         |         | $BSb=1.0/(2*B*Sbias)$                      |
|         | $C=2.5e-5$      |         | $GamaN=azV*Sbias+1I\_e$                    |
|         | $t\_r=7.772e-9$ |         | $Nbias=(G*Sbias+Ib)/(e1*azV*Sbias+e1I\_e)$ |

Figure 2. Parameters used in the circuit model

Rate equations have various levels of complexity to express more accurate laser operations. The presented model is one of the simplest equivalent circuit models. In other words, more complex equations and many parameters are required to improve model's performance. The main problem with the rate equation-based model is that circuit designers need to know the physical fabrication parameters of the laser, which includes the volume of the active region. Although laser manufacturers provide such data, it is typically limited and insufficient for the circuit design. In addition, the remaining parameters still need a lot of measurement facilities and a long measurement time [4]. Finally, rate equation-based models could have an advantage in expressing nonlinear characteristics like near threshold operation; which are critical for OEIC design due to the slow speed and signal distortion from operation in the nonlinear region [4].

### 3.2 Circuit model of small signal modulation

Small signal modulation components are  $S_m$  and  $N_m$ , which can be derived from Eqs. (12) and (13) and multiplying both equations by e:

$$\begin{bmatrix} e(\Gamma_S + j\Omega_m) & -e \frac{a\zeta}{V} \left( S_b + \frac{CV}{a\zeta\tau_r} \right) \\ eA_b & e(\Gamma_N + j\Omega_m) \end{bmatrix} \begin{bmatrix} S_m \\ N_m \end{bmatrix} = \begin{bmatrix} 0 \\ I_m \end{bmatrix} \quad (22)$$

These nodal voltage equations identically describe the relations of the circuits shown in Fig. 3(a) and 3(b), therefore analysis of the circuits with software such as ADS should lead to analogous results obtained from the numerical simulation of rate equations.

According to the nodal voltage equations, diagonal elements of nodal admittance matrix in Eq. (22) specify the admittance between corresponding node and ground, while because of non-equal expression in the off-diagonal entries of the matrix, there is no component placed between nodes  $S_m$  and  $N_m$ . These expressions can be modeled as voltage-controlled-current-sources (VCCS).

Identical to bias components there is two nodes ( $S_m$  and  $N_m$ ) corresponding to small-signal parameters. Thus each element of the matrix is an admittance attached to nodes. At this moment it is expected to introduce them. The first expression is  $e\Gamma_s$  which can be obtained from Eqs. (10) and (15). Equation (10) can be rewritten as:

$$\frac{CN_b}{\tau_r S_b} = BS_b - A_b + G_{th} \quad (23)$$

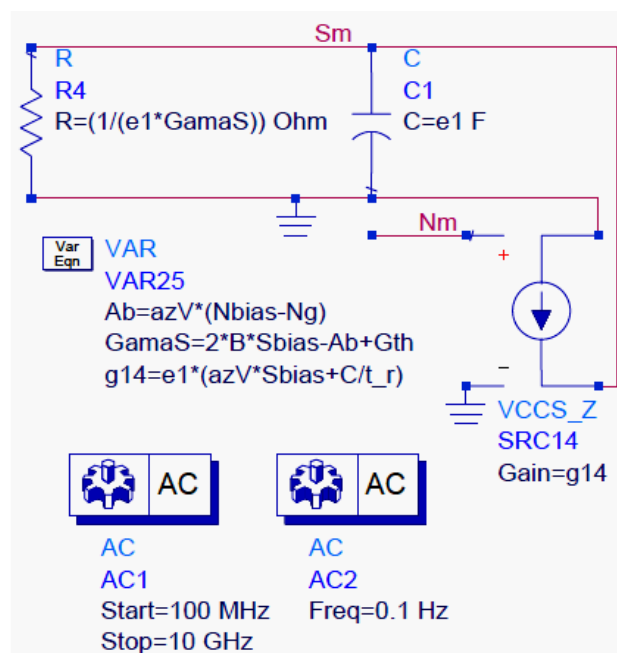
Now it can be substituted in Eq. (15) then multiplied by 'e' as well, produce expanded form of  $e\Gamma_s$  in the first entry of the matrix as:

$$e\Gamma_s = e(2BS_b - A_b + G_{th}) \quad (24)$$

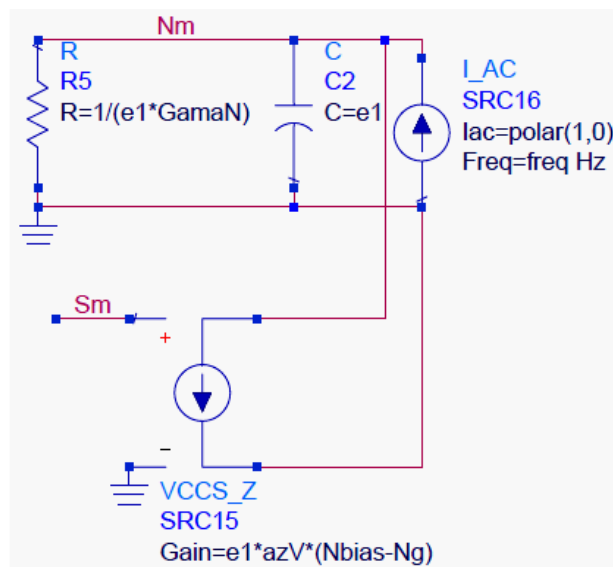
To derive a lumped-element small signal equivalent circuit model, several theoretical components should be defined.

As the matrix is naturally admittance, all entries of the matrix are also admittance. So Eq. (24) is reverse value of R4. The expression  $ej\Omega_m$  appeared in the 1st and 4th entries of the matrix can be modeled as the capacitor C1 with the capacitance value of 'e' ( $1.6 \times 10^{-19}$ ). Moreover the term  $-ea\zeta/V(S_b + CV/(a\zeta\tau_r))$  which is multiplied by  $N_m$ , can be modeled as voltage-controlled current source SRC14.

The equivalent circuit model of small-signal semiconductor laser is illustrated in Figure 3 [8-11].



(a)



(b)

Figure 3. Actual schematic implementation for small signal parameters; (a)  $S_m$  and (b)  $N_m$

According to the second row of the matrix, there are two parameters left to be identified. One is  $A_b$  which can be obtained from Eq. (14) and is modeled as the voltage-controlled current source SRC15; the other parameter is  $e\Gamma_N$  which is simply modeled as resistor  $R_5$  using the Eq. (16).

The term  $I_m$  in the right side of Eq. (22) is the magnitude of the corresponding small-signal perturbation and is modeled as an AC current source SRC16 with amplitude 1 and phase 0. As mentioned before capacitor C2 is represented for the term  $ej\Omega_m$ .

At a given bias current  $I_b$ , the modulation response  $H_m(\Omega_m)$  at a specified modulation frequency  $\Omega_m$  is defined as the ratio of the modulated photon number  $S_m(\Omega_m)$  to the corresponding un-modulated value  $S_m(0)$  [6, 9-11].

$$H(\Omega_m) = \frac{S_m(\Omega_m)}{S_m(0)} \quad (25)$$

To achieve the transfer function of Eq. (25), the circuit has been simulated with two conditions. These conditions are symbolized by two AC simulation components in the ADS software which is shown in Figure 3(a). The first one (AC1) simulates the numerator of the transfer function with frequency sweep from 100 MHz to 10GHz, and the other (AC2) corresponds to the denominator of transfer function which sets in the frequency near zero. After simulating the circuit to plot the function, the expression in Eq. (26) is used.

$$(dB(AC1.AC.Sm)-dB(AC2.AC.Sm))/2 \quad (26)$$

At which the 1/2 is used for transforming default dB function ( $20 \log x$ ) to ( $10 \log x$ ). The result of this simulation is shown in Figure 4 which is conformed to the result of numerical simulation done with MATLAB software illustrated in Figure 5.

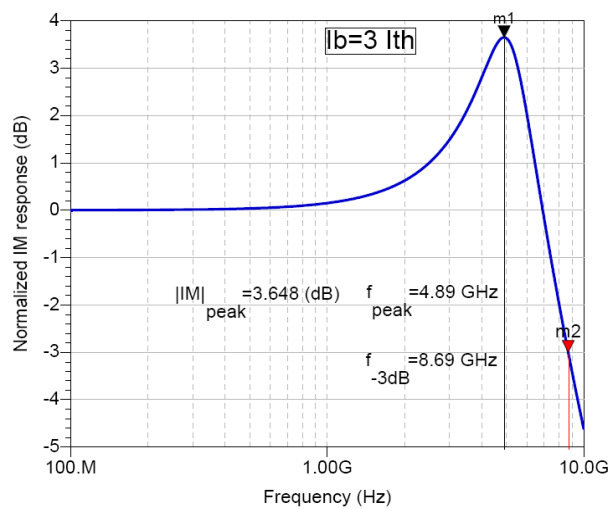


Figure 4. Modulation response obtained from the simulation of the circuit model with ADS software

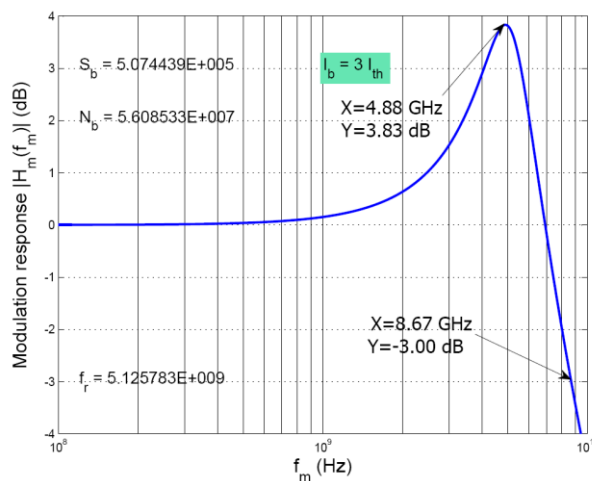
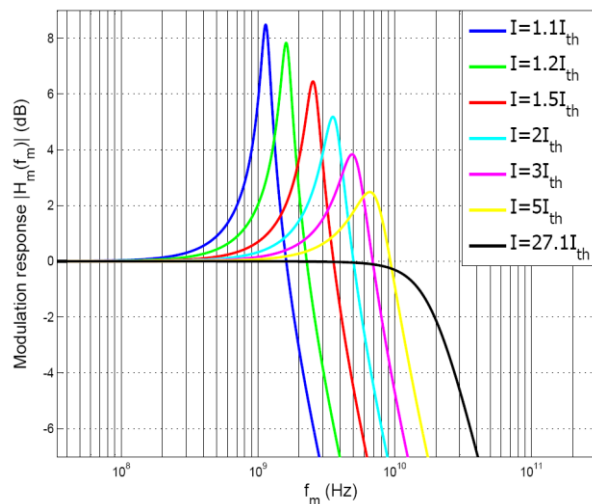


Figure 5. Result of numerical simulation with MATLAB software

These figures plot frequency spectrum of the modulation response  $|H_m(f_m)|$  when  $I_b = 3 * I_{th}$ . The figures show that  $|H_m(f_m)|$  exhibits a pronounced peak at the frequency  $f_m(\text{peak}) = 4.9$  GHz. In this case, the modulation bandwidth is  $f_{3\text{dB}} = 8.69$  GHz. for more details on this behavior refer to section 3.1 of the reference [6].

#### IV. RESULTS AND DISCUSSION

Variation of the response  $|H_m(f_m)|$  with the bias current  $I_b$  is shown in Figure 6.  $I_b$  changes from  $I_b = 1.1 * I_{th}$  to  $I_b = 27.1 * I_{th}$  which corresponds to  $f_{3\text{dB}}(\text{max})$ . The spectra exhibit the common feature that the low-frequency components are flat with  $|H_m(f_m)| = 1$ . Figure 6 shows that the peak value  $|H_m(\text{peak})|$  decreases with the increase of  $I_b$ , and the spectrum becomes flat when  $I_b = 27.1I_{th}$ .



**Figure 6.** Variation of  $|H_m(f_m)|$  with bias current  $I_b$  acquired from simulation with MATLAB

Sweeping the coefficient  $k$  in relation  $I_b = k * I_{th}$  is accomplished with the tuning capability of ADS software and the result is shown in Fig. 7.

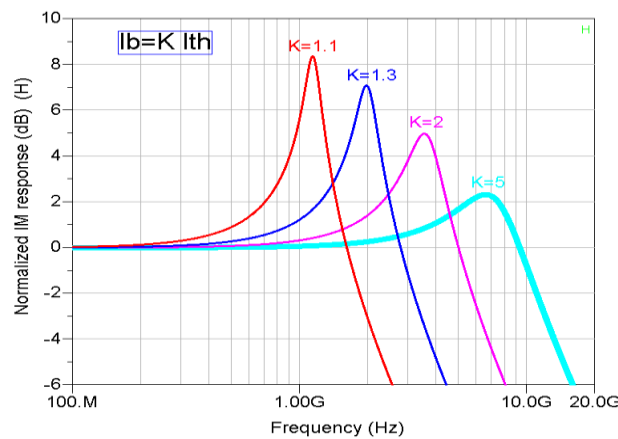


**Figure 7.** 4 responses of  $|H_m(f_m)|$  acquired from circuit simulation with ADS

Figure 8 is generated by defining Eqn. Max1 for better vision on relation between increase of  $I_b = k * I_{th}$  and reduction of the peak value of the modulation response.

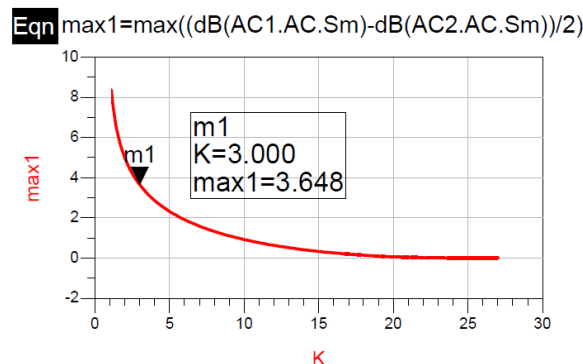


**Figure 8.** Variation of  $|H_m(f_m)|$  with bias current  $I_b$

The gain suppression term  $BS_b$  increases with the photon number  $S_b$ , and consequently with  $I_b$ . Here, we illustrate the influence of gain suppression on the modulation characteristics by varying the nonlinear gain coefficient  $B$  relative to its value  $B_0$ . Figure 9 plots the modulation response  $|H_m(f_m)|$  as

a function of  $B$  when  $I_b = 3I_{th}$ . It shows that when  $I_b = 3I_{th}$ , increase of gain suppression  $B$  from 0 to  $3B_0$  gradually decrease the spectra around  $f_m(\text{peak})$ .

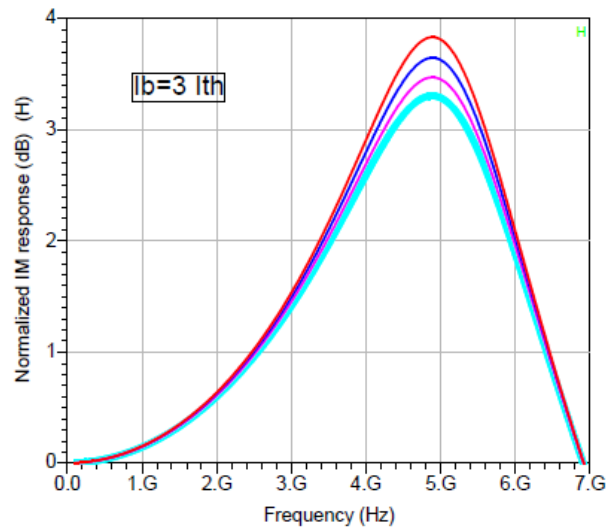


Figure 9. Decrease of  $|H_m(f_m)|$  with increase of gain suppression  $B$

## V. CONCLUSIONS

In this paper, the SL's equivalent circuit model was developed based on simple rate-equations which utilize an AC current source to account for the small signal perturbation. The comparison in Section 4 showed that our model was useful for describing the SL's small signal characteristics taking account of gain suppression.

Just as mentioned before, such a model is very helpful in the simulation and design of optoelectronic systems with SLs. By implementing the SPICE-like equivalent circuit models it can be conveniently combined with the electrical components in large-scale EDA designs.

## REFERENCES

- [1] R. Ramaswamy, K. Sivarajan, G. Sasaki, (2008) "Optical Networks: A Practical Perspective", Morgan Kaufmann, Third Edition.
- [2] S. W. Z. Mahmoud, (2007) "Influence of gain suppression on static and dynamic characteristics of laser diodes under digital modulation", *Egypt. J. Sol.*, Vol. 30, No. 2, pp. 237-251.
- [3] M. Ahmed, M. Yamada, (2012) "Modeling and simulation of dispersion-limited fiber communication systems employing directly modulated laser diodes", *Indian J. Phys.*, Vol. 86, No. 11, pp. 1013-1020
- [4] J. H. Kim, (2005) "Wide-Band and Scalable Equivalent Circuit Model for Multiple Quantum Well Laser Diodes", Ph.D. dissertation, Georgia Institute of Technology.
- [5] J. Gao, X. Li, J. Flucke, G. Boeck, "Direct parameter-extraction method for laser diode rate-equation model", (2004) *J. Lightwave Technol.*, Vol. 22, No. 6, pp. 1604-1609
- [6] M. Ahmed, A. Ellafi, (2008) "Analysis of small-signal intensity modulation of semiconductor lasers taking account of gain suppression", *Pramana - Journal of Physics*, Vol. 71, No. 1, pp. 99-115.
- [7] M. F. Ahmed, S. W. Z. Mahmoud, M. Yamada, (2003). "Influence of the spectral gain suppression on the intensities of longitudinal modes in 1.55  $\mu\text{m}$  InGaAsP lasers", *Egypt. J. Sol.*, Vol. 26, No. 2, pp. 205-224.
- [8] K. Abedi, and M. B. Nasrollahnejad, "Analysis and Circuit Model of Optical Injection-Locked Semiconductor Lasers," *IREMOS*, Vol. 4, No. 4, pp. 1988-1991, 2011.
- [9] M. Ahmed, and M. Yamada, "Mode oscillation and harmonic distortions associated with sinusoidal modulation of semiconductor lasers," *European Physical Journal D*, Vol. 66, No. 9, pp. 246-1,246-9, 2012.
- [10] S. Odermatt, B. Eitzigmann, and B. Schmithuse, "Harmonic balance analysis for semiconductor lasers under large-signal modulation," *Opt. Quant. Electron.*, Vol. 38, pp. 1039-1044, 2006.
- [11] B. Schmithüsen, S. Odermatt, and B. Witzigmann, "Large-signal simulation of semiconductor lasers on device level: numerical aspects of the harmonic balance method," *Opt. Quant. Electron.*, Vol. 40, No. 5-6, pp. 355-360, 2008.

## AUTHOR

**Kambiz Abedi** was born in Ahar, Iran, in 1970. He received his B.S. degree from University of Tehran, Iran, in 1992, his M.S. degree from Iran University of Science and Technology, Tehran, Iran in 1995, and his Ph.D. degree from Tarbiat Modares University, Tehran, Iran, in 2008, all in electrical engineering. His research interests include design, circuit modeling and numerical simulation of optoelectronic devices, semiconductor lasers, optical modulators, optical amplifiers and detectors. Dr. Abedi is currently an Assistant Professor at Shahid Beheshti University, Tehran, Iran.



**Mohsen Khanzadeh** was born in Bafgh, Iran, on August 12, 1980. He received the B.S. degree in electronics engineering from Guilan University, Rasht, Iran, in 2003, and is currently working toward the M.S. degree in electrical engineering at the University of Shahid Beheshti, Tehran, Iran. He worked on equivalent circuit model of LASER devices design and analysis. His research interests are optical fiber communication and modeling of the SLs.

